


Numerical investigation and modelling of controllable parameters on the photovoltaic thermal collector efficiency in semi-humid climatic conditions

Ilias Terrab, Nor Rebah, Samir Abdelouahed, Michel Aillerie & Jean-Pierre Charles



To cite this article: Ilias Terrab, Nor Rebah, Samir Abdelouahed, Michel Aillerie & Jean-Pierre Charles (2022) Numerical investigation and modelling of controllable parameters on the photovoltaic thermal collector efficiency in semi-humid climatic conditions, Energy Sources, Part A: Recovery, Utilization, and Environmental Effects, 44:4, 8760-8776, DOI: [10.1080/15567036.2022.2125124](https://doi.org/10.1080/15567036.2022.2125124)

To link to this article: <https://doi.org/10.1080/15567036.2022.2125124>

 View supplementary material 

 Published online: 20 Sep 2022.

 Submit your article to this journal 

 View related articles 

 View Crossmark data 



Numerical investigation and modelling of controllable parameters on the photovoltaic thermal collector efficiency in semi-humid climatic conditions

Ilias Terrab^a, Nor Rebah^a, Samir Abdelouahed^a, Michel Aillerie^b, and Jean-Pierre Charles^b

^aLaboratoire de Physique de La Matière Et du Rayonnement, Département de Physique, Université Mohamed-Chérif Messaadia - Souk Ahras, 41000, Souk Ahras, Algeria; ^bLaboratoire Matériaux optiques, Photoniques et Systèmes, LMOPS, Matériaux, Composants et Systèmes Photovoltaïques (MCS-PV), Université de Lorraine, Metz, France

ABSTRACT

Hybrid Photovoltaic Thermal (PV/T) systems are energy-generation systems that transform thermal irradiance into both electrical and thermal energy at the same time. Hybrid photovoltaic thermal systems consist of a photovoltaic panel connected to a thermal collector. The main objective of this paper is to find the optimal operating conditions that can be controlled to decrease the photovoltaic panel temperature in order to improve the electrical and thermal performance of PV/T systems. In this work, we proposed the 3D numerical model that is implemented within the COMSOL Multiphysics program to study the PV/T system. The experimental input data being used in this research study reflects a typical Algerian area with semi-humid climate conditions. We study the effect of water velocity, pipe length, diameter, thickness and inlet fluid temperature on the electrical and thermal performance using the design of experiments (DOE) method. Further, the analysis of variance (ANOVA) is used to identify which of these effects impact the most the photovoltaic thermal and electrical efficiencies, the response surface methodology (RSM) is employed to describe how these effects are interacting. Based on ANOVA analysis, the following factors are reported to be important: water velocity, pipe diameter, pipe length and the inlet fluid temperature. Further, there is a significant interactions between water velocity, pipe length and pipe diameter. Among the operating conditions being calculated using the RSM, the optimal one is found when water velocity, pipe length, pipe diameter, pipe thickness and inlet water temperature have the following values, 0.05 m/s, 7.27 m, 0.01 m, 0.0008 m and 10°C, respectively. The corresponding thermal, electrical and overall efficiency were found around 80.73%, 12.87% and 93.60%, respectively. The proposed simulation model provides a reliable framework to study, improve and predict PV/T systems performance whilst ensuring low computational time.

ARTICLE HISTORY



Received 3 January 2022
Revised 1 September 2022
Accepted 6 September 2022


KEYWORDS

Photovoltaic thermal system; 3D numerical model; finite element method; response surface methodology; solar energy

Introduction

The use of renewable energies as energy resources is the most reliable solution to meet the global expectation of energy supply due to the growing demand across the world as well as the scarcity and the exhaustible character of fossil resources (Kalkan and Akif 2019). Not to mention the harmful effects on the climate and the environment due to the excessive use of conventional fuel. Thus, the search for another source of clean energy is becoming a paramount concern for policy makers. In this context, solar energy comes on top of all renewable energies given its availability, abundance,

CONTACT Ilias Terrab  i.terrab@univ-soukahras.dz  Laboratoire de Physique de La Matière Et du Rayonnement, Département de Physique, Université Mohamed-Chérif Messaadia - Souk Ahras, 41000, Souk Ahras, Algeria

 Supplemental data for this article can be accessed online at <https://doi.org/10.1080/15567036.2022.2125124>

sustainability and cost-free nature. In addition to that, thanks to its thermal and optical character of energy, the sun has the potential to satisfy a considerable portion of humanity's energy needs (Kalkan and Akif 2019), under two forms: temperature and electricity (Afroza et al. 2019) that are very useful for applications in all areas (including industrial and domestic usage). As a result, several research studies for the promotion of the use of this energy are being carried out more and more in recent years, especially, those related to solar thermal and electrical systems, which provide us with the most efficient and practical way to capture and transform solar energy into thermal and electrical energy.

Photovoltaic (PV) systems are essential for producing power from sunshine (Kalkan and Akif 2019). However, only 15% to 20% (Fazlay et al. 2020) of solar radiation is transformed into electricity by PV panels (Rahman, Hasanuzzaman, and Rahim 2015) with the remainder part dissipating as heat or reflected (Marudaipillai et al. 2020). This dissipated heat increases the solar cells temperature which reduce the electrical efficiency (A. Antony, Wang, and Roskilly 2019).

Nevertheless, temperature and optical radiation have antagonist effects on the efficiency of the sensor systems such as photovoltaic (PV) cells, panels or more generally modules. According to the literature, the electrical efficiency of current PV Silicon based modules decreases by 0.45 to 0.50% (Fazlay et al. 2020) for each degree of increase in the temperature of the module above 25°C (Brahim and Jemni 2017). This may alter 20% of the device performance. Therefore, cooling the PV panel is very important to increase system efficiency and protect it from overheating which can damage the system (Fazlay et al. 2020).

One of the solutions to this problem is to integrate a thermal panel into the PV system to have a hybrid photovoltaic/thermal (PV/T) system. In this way, this hybrid system can take advantage of a PV sensor for the production of electricity, heating a fluid which will be the temperature transport vector for the PV part, decreasing its temperature and thus increasing its produced electrical energy (Abdelrazik et al. 2018).

This photovoltaic-thermal hybrid system, which combines the collection of thermal energy and the radiative transformation for the production of electrical energy, is a promising solution for a better exploitation of solar energy either to heat a fluid to have thermal energy or to increase electrical efficiency. Furthermore, the efficiency of a PV panel with a thermal panel (PV/T) is by far much better than the one without a thermal panel (Ben Cheikh El Hocine, Gama, and Touafek 2018).

On the other hand, photovoltaic/thermal (PV/T) systems, are intended to remove surplus heat from PV panels by employing a cooling system such as air or water (Kalkan and Akif 2019). A hybrid photovoltaic thermal system is a solar energy system that is designed to convert solar energy into both electricity and heat (Abdullah et al. 2019). PV/T combines a PV panel which produces electricity from a short wave radiation and a thermal collector that gathers thermal energy from a long wave solar radiation (Lateef et al. 2020).

From the research literature, a general topology of PV/T is based on different thermal collector, PV panel, working fluid, glazing and thermal absorber (Herez et al. 2020).

One of the main advantages of PV/T systems is the high performance unit surface area as compared to the performance of a PV panel and thermal collector separately. This means that the lower the area of the surface, the better is the performance of the PV/T, leading to a considerable reduction of the installation cost (Touafek, Haddadi, and Malek 2013).

There are three types of factors and parameters that influence the performance of PV/T systems: climatic parameters (solar radiation, wind speed.) (Sachit et al. 2018), operational parameters (velocity, inlet water temperature.) (Deng et al. 2020) and design parameters (pipe diameter, pipe thickness, . . .) (Shuang-Ying et al. 2011). Since the invention of the PV/T in 1970, several theoretical and experimental investigations were published studying novel designs of PV/T collectors (Afroza et al. 2019).

In the work of (Rejeb et al. 2020), the parallel plate of a thermal collector is attached to the backside of the PV module without an absorber plate using a thermal paste (Rejeb et al. 2020). The authors found that the PV/T efficiency was nearly the same with and without any absorber plate. (Moradi Kamran, Ebadian, and Xian Lin 2013) studied the effects of the control factors on the PV/T efficiencies. (Rahman, Hasanuzzaman, and Rahim 2015) assessed the impact of the cooling water

flow rate on the PV/T module efficiency. (Jonas et al. 2019) studied the influence of a number of variables representing several factors on the efficiency of the PV/T system using TRNSYS software simulations to validate the model. Numan et al. (Numan and Kaya 2020) studied the performance of a PV/T system using different types of fins materials and configurations. Using the Taguchi method, they found the best combination of parameters affecting thermal and electrical efficiencies. Investigating the effect of operational factors on the performance of the PV/T system by the response surface methodology (RSM), (Rejeb et al. 2020) established a novel statistical model. (Sathyamurthy and Sharshir 2020) reviewed and investigated recent cooling systems for PV. They classified them according to heat transfer modes (convective, conductive and radiative cooling). (Ramdani and Ould-Lahoucine 2020) introduced a new concept to simulate a water-based hybrid photovoltaic thermal collector. Using ANSYS Fluent software, they suggested superimposing a layer of water on top of the PV module to cool the PV cells while filtering the incoming solar radiation. (Das and Kalita 2020) presented two distinct PV/T collector designs, the first with a copper absorber plate on the back of PV panels and the second with a tube for fluid flow. (Sainthiya and Singh Beniwal 2020) studied the efficiency of the PV model for two types of cooling systems (with and without water cooling) as well as four distinct flow rates.

Improving the performance of PV/T systems by changing the design configuration (e.g., channel height, number of fins and passes) and/or heat transfer fluid (HTF) operating conditions (eg, inlet temperature and mass flow rate) is being increasingly important in recent years. (Kalkan and Akif 2019) proposed a PV/T system that uses air as a cooling system using RSM and fluid dynamics (CFD) solver as implemented in ANSYS-FLUENT. The consequences of modifying a wide range of design factors, operational situations and meteorological data are studied and the system's best conditions are determined. The results showed that the channel height and air velocity affect the overall efficiency and the air output temperature of the PV/T. The optimal conditions were obtained for a collector with a length of 1.5 m, a channel height of 1 cm and an air velocity of 2.3 m/s. (Kazemian, Khatibi, and Ma 2021) developed a PVT system with phase change material (PV/T/PCM), where they used RSM to find the best condition for various responses. PCM layer thickness, solar irradiation, PCM melting temperature and ambient temperature were chosen as operational factors. Electrical power, thermal power, electrical exergy, thermal exergy and entropy formation were the five studied responses. The results revealed that solar irradiation has the biggest influence on energy and exergy outputs and that the ideal operating conditions were found to be: a 1.5 cm thick PCM layer, a solar irradiation of 901 W/m² and a melting temperature of 25°C. (Pang et al. 2021) discussed the influence of cross-sectional geometries, the size and the spacing ratios on the performance of a PVT system. They have shown that solar irradiation raises the PV/T temperature while fluid flow has a negative influence on the PV/T temperature. In another paper by (Kazemian et al. 2021), a novel system formed by connecting a solar collector in series with a photovoltaic thermal module was proposed. In their work, the Taguchi method was used to assess the operating conditions values of mass flow rate, solar irradiation, coolant inlet temperature, ambient temperature and wind speed. The corresponding factorial parameters were found to be of 50 kg/h, 1000 W/m², 24°C, 28°C and 1 m/s, respectively. MATLAB software was used by (Valeriu et al. 2022) to optimize the effect of velocity and water film thickness on the heat exchange and the PV/T performance. The water velocity and film thickness were found to have a positive effect on heat transfer with optimal values of 0.035 m/s and 7 mm, respectively. The corresponding thermal and electrical efficiencies were found of 1334.5 W and 316.56 W, respectively, at an inlet temperature of 20 C. The effect of the parallel cooling channel on the thermal performance of the photovoltaic thermal collector was discussed by (Shen et al. 2021). The influence of the number of sub-channels, the configuration of the inlet and outlet and the diameter ratio between the main channel and the sub-channels were studied within the same work. Authors found that using 10 parallel channels and increasing the diameter ratio between the main channel and that of the sub-channels from $D/d = 2$ to $D/d = 4$ lead to the PV/T best efficiency. (Gelis et al. 2022) designed a new cooling system of 12 cooling blocks. Which are put on the back surface of the PV panel to lower the panel's temperature. The authors investigated the performance of the proposed design using factorial design. They found that

the electrical efficiency reaches 17.69% at the optimal conditions of 900 W/m^2 of solar irradiation and 1.65 L/min of volumetric flow rate. The thermal efficiency reaches 58.5% at 900 W/m^2 of solar irradiation and 0.55 L/min of volumetric flow rate. (Gomaa, Ahmed, and Rezk 2022) addressed the impact of solar irradiation and cooling water flow rate on the performance of the PV/T with thin and thick (3 mm and 15 mm) cooling cross-fined channel boxes. They revealed that 1000 W/m^2 and 3 L/min are the optimal conditions for both thin and thick box heat exchangers.

To the best knowledge of the authors, there is a dearth of research studies which investigated the association and the number of parameters that we have chosen for the study of the optimization of the PV/T. This is besides the exploratory studies concerning the impact of these parameters relative to each other for estimating the efficiency of the system. Another novelty of this work is that factors related to the cooling system (serpentine) such as the length, diameter and thickness of the tube have not been dealt with previously. Also, the development of a novel quadratic equation for forecasting the electrical and thermal efficiency of a photovoltaic thermal system based on the input parameters investigated and the 3D numerical model of PVT systems that takes into account all different layers of the PVT unit has been studied and for the first time has been done with the climatic condition of Souk Ahras.

In our work, the factorial parameters corresponding to water velocity (A), pipe length (B), pipe diameter (C), pipe thickness (D) and inlet fluid temperature (E) are studied. A PV/T panel model is designed using the finite element method as implemented in COMSOL Multiphysics in the first step. Then, the effects of the most relevant factorial parameters on electrical and thermal efficiencies are assessed using the Design of Experiments Method (DOE) and ANOVA. Finally, using the RSM which is implemented within the Minitab software, an optimization process is carried out to find the best operating conditions. Indeed, changing the different factorial parameters to get the optimal efficiencies provided us with the corresponding optimal water velocity (A), the optimal pipe diameter (C), the optimal pipe length (B), thickness (D) and the optimal inlet fluid temperature (E).

Methodology

COMSOL modelling

PV/T solar panel description

PV/T system consists of two principal models: a PV model and a solar collector model. The PV model characteristics being used as inputs in our calculations are those of the one installed in our laboratory. This is a typical model which is made of monocrystalline silicon cells with an electrical efficiency of 14.47%. Sheet and tube collectors are attached to the PV panel in order to refrigerate solar cells and collect thermal energy.

The PV/T solar panel layers include the front cover (glass), encapsulation (ethyl vinyl acetate (EVA)), PV cells, back sheet (Tedlar) and a thermal paste as a heat conductor as shown in Figure 1 (Nahar, Hasanuzzaman, and Rahim 2017b). The sheet and tube collector are made of the flow channel

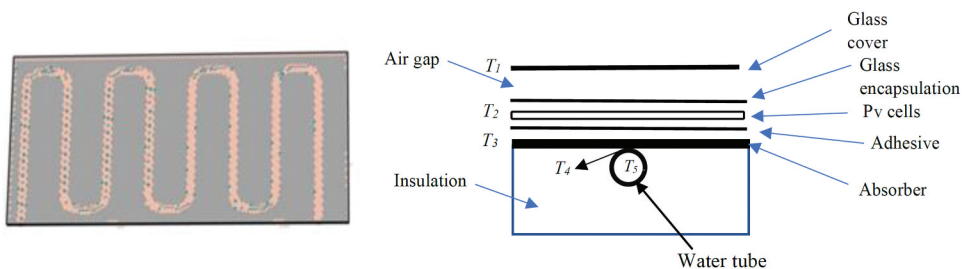


Figure 1. PV/T collector with typical sheet-and-tube design (da Silva and Fernandes 2010).

in serpentine form with a single pass with two regions: fluid region (water) and solid region (copper) where the choice of copper is due to its high thermal conductivity.

Heat transfer equations

Heat transfer in PV/T occurs by conduction from the surface of the cell to the flow channel where the thermal energy is carried by particles vibration (Nahar, Hasanuzzaman, and Rahim 2017a).

COMSOL uses Fourier's law of heat conduction to solve the heat transfer equation:

$$\nabla \cdot (k \nabla T) = 0 \quad [1]$$

Where T is the temperature and k is the thermal conductivity.

Inside the channel, the heat is carried by the fluid flow and is either transferred by conduction or convection (Leonzio 2019; Nahar, Hasanuzzaman, and Rahim 2017b). In such channel, the fluid is considered as an incompressible Newtonian fluid where its flow is steady. This flow is governed by the following equations (Fontenault and Gutierrez-Miravete 2012):

$$\nabla \cdot (\rho u) = 0 \quad [2]$$

$$P(u \cdot \nabla)u = -\nabla P \quad [3]$$

Thermal model

Numerical simulation is the most effective approach to analyze and optimize thermal and electrical efficiency. Our study is based on the following assumptions:

- The solar irradiation on the whole PV/T panel is the same.
- There is no dust or impurities on the PV/T surface that reduce the PV absorption factor.
- The coolant inlet water has a uniform temperature.
- The flow of inlet water is incompressible and laminar.
- The variation of temperature anywhere along the PV/T layer is negligible.
- The bottom side of the absorber channel is considered to be isothermal.
- The transmissivity of ethyl vinyl acetate (EVA) is estimated to be about 100%.

The materials and thermal characteristics in addition to the PV dimension and design requirements are outlined in Tables 1 and 2.

Table 1. Material and thermal characteristics of the PV/T collector.

Materials	Layer	Thermal Density [kg/m ³]	Thermal Conductivity [W/(mK)]	Heat capacity at constant pressure [J/kg K]	Thickness (mm)
Glass	Top cover	2210	1.4	730	3
EVA	Encapsulant	950	1	1	0.8
Silicon	Solar cell	2329	130	700	0.1
Tedlar	Bottom cover	1190	0.18	1470	0.05
Thermal paste	Conductor	63	1.9	2000	0.03

Table 2. Characteristics of the PV module.

Item	Values
Cell material	p-Si monocrystalline
Size of the PV module	1205 mm×545 mm
Size of cell	125mm x 125mm
Number of cells	36 cells in a series
Module Efficiency	14.47%

The following formula can be used to calculate the total amount of energy (solar irradiance) falling on a PV module (Fontenault and Gutierrez-Miravete 2012; Nahar, Hasanuzzaman, and Rahim 2017a; Obalanlege et al. 2019):

$$E_c = P_c \tau_g \alpha_c R A_c \quad [4]$$

The thermal energy obtained from coolant water is described as follows:

$$E_{th} = \dot{m} C_{pW} (T_{out} - T_{in}) \quad [5]$$

The following equation is used to calculate the mass flow rate (\dot{m}):

$$\dot{m} = \rho U_0 A_{fc} \quad [6]$$

Where A_{fc} is the inlet velocity per unit cross-sectional area, which is defined as:

$$A_{fc} = \pi \frac{D_i^2}{4} \quad [7]$$

Where D_i is the tube inner diameter.

The PV/T thermal efficiency is defined as:

$$\eta_{th} = \frac{E_{th}}{E_c} \quad [8]$$

Electrical model

The following equation is used to calculate the electrical efficiency (Dutreuil and Hadim 2017; Tata, Feddaoui, and Belkassmi 2018):

$$\eta_{el} = \eta_{Tref} \left[1 - \beta_{ref} (T_c - T_{ref}) \right] \quad [9]$$

Where T_{ref} is the reference cell temperature at standard conditions for the city of Souk Ahras in Algeria with the geographical coordinates of: 36° 17' 15" north and 7° 57' 15" east. The climate for the region of Souk Ahras is semi-humid with the following parameters ($R = 1400 \text{ W/m}^2$ and $T_{ref} = 25 \text{ }^\circ\text{C}$). β_{ref} is the temperature coefficient at the cell reference temperature. This coefficient depends on the PV module materials. In the Equation [9], the value of β_{ref} is set as 0.00041/K for silicon cell (Ben Cheikh El Hocine, Gama, and Touafek 2018).

The PV/T collector total efficiency is calculated as:

$$\eta_{tot} = \frac{E_{th} + E_{el}}{E_c} \quad [10]$$

Where the total amount of the electrical energy required by the PV cells (E_{el}) can be expressed as:

$$E_{el} = \eta_{el} E_c \quad [11]$$

Boundary conditions

The following boundary conditions for the heat transfer equations used to solve partial differential equations. At the top of the surface:

$$-k_s \frac{\partial T_s}{\partial z} = q = h_c (T_{amb} - T_s) \quad [12]$$

At the solid-fluid interface: (no slip condition)

$$\mathbf{u} = \mathbf{w} = \mathbf{U} = 0 \quad [13]$$

$$\left(\frac{\partial T_s}{\partial n}\right)_{\text{fluid}} = \frac{k_s}{k_w} \left(\frac{\partial T_s}{\partial n}\right)_{\text{solid}} \left(\frac{\partial T_s}{\partial n}\right)_{\text{fluid}} = \frac{k_s}{k_w} \left(\frac{\partial T_s}{\partial n}\right)_{\text{solid}} \quad [14]$$

Where k_s and k_w represent the thermal conductivity for the solid and water, respectively.
At the channel inlet:

$$\mathbf{U} = \mathbf{U}_0, \mathbf{u} = \mathbf{w} = 0 \quad [15]$$

$$T = T_{\text{in}} \quad [16]$$

At the channel outlet:

$$P = 0 \quad [17]$$

Mesh generation

The mesh generation is the numerical approach used to solve the partial differential equations (“Detailed Explanation of the Finite Element Method FEM” n.d). The finite element method separates a complex structure into smaller and simpler sections known as finite elements. The PV/T is meshed using the built-in environment mesh sequence as implemented in COMSOL Multiphysics. At each border, the number of mesh elements increases, leading to a more accurate heat transfer and flow calculations. Free tetrahedral settings were used to develop this model (“Detailed Explanation of the Finite Element Method FEM” n.d).

The free tetrahedral method is used to generate the meshing grid. To make sure that the convergence is achieved, 100,785 to 331,206 elements were used. It is observed that starting from 105,403 elements, a good convergence is achieved as the computational accuracy is reached. The maximum element size is 0.121 m, the smallest element size is 0.0217 m, the maximum element growth rate is 1.5, the curvature factor is 0.6 and the narrow region resolution is 0.5.

Design of experiments methodology (DOE)

The design of experiments (DOE) is a computational approach that is usually used to assess the relationship between the variables that influence a process output. In our case, we used it to identify which factors and how these factors influence the efficiency process. In other words, it is used to explain what causes what by exploring the effects of covariate factors (Montgomery 2005). DOE is also utilized to learn about a system, process, or product and estimate its optimal operating conditions.

The main advantages of DOE are:

- Obtain an optimal solution by studying different factors at the same time leading to a decrease in the number of real experiments and tests.
- Improve the accuracy of the results by running different DOEs at an affordable computational time cost.
- Studying the interactions and correlations between factors (Montgomery 2005).

ANOVA modeling

The analysis of variance (ANOVA) is an analytical technique for determining whether two or more factors differ significantly. ANOVA checks the means of several samples to determine the impact of one or more variables (Leonzio 2019). In this analysis, using experimental error (σ_ϵ), we determine

significant effects and interactions between factors. The tracking of these factors and all relevant interactions and effects is assessed by Yates's algorithm using Minitab 16.

To assess statistical significance, the F-value (Fischer variance ratio) and p -value (significant probability value) are calculated. The probability value within the 95% confidence interval (or 5% significance level) is used to accept or reject some model terms (Montgomery 2005).

Response surface methodology

Response surface methodology (RSM) is an approach that was proposed in the mid-1950s by Box and Wilson (1951) (Dutta 2017; Geiger and Algorithm n.d). RSM is a well-known optimization method to determine, approximate and optimize the stochastic models. The first step in RSM is to determine a reasonable estimate of the true relation between the response and the independent variables. Considering the response as process and the involved variables as factors/effects, this first step is achieved by running a sequence of DoEs. After having identified a response Y to a set of factors/variables X_i , the following second-order polynomial model (Khuri and Mukhopadhyay 2010) is used to assess the response Y to the various variables X_i in the following way:

$$Y = a_0 + \sum_{i=1}^3 a_{ii}X_iX_i + \sum_{i < j}^3 a_{ij}X_iX_j \quad [18]$$

Where X_i and X_j are the design variables and a_{ij} are the tuning parameters (Deng et al. 2020; Terrab and Kara 2018).

Results and discussion

The DOE proposed by Taguchi is a new approach adopted in order to decrease the simulation time needed to optimize the PV/T controlling parameters (Numan and Kaya 2020). While an optimal design needs fewer experiments compared to the non-optimal one (J. Antony 2015), the results obtained in both cases have the same accuracy. The results are consistent across the full sequence of the DOE experiments. These results are only affected by the initial variables and settings. Table 3 shows the controllable variables (the water velocity, pipe length, diameter, thickness, and inlet fluid temperature). The levels of these factors are planned in advance. In fact, the lower (-) and upper (+) levels, representing the minimum and maximum values, respectively, were carefully determined by taking only relevant intervals for factors, resulting in considerable variations of efficiency. This method decreases the performed simulation time.

The studied PV/T configurations and the corresponding results of thermal and electrical efficiency are indicated in Table 1 within the Appendix section. The values reported in this table were calculated using equations 8 and 9. Indeed, we used COMSOL to calculate T_{out} and T_c for a given T_{in} . Then, using equations 8 and 9, we calculated electrical and thermal efficiencies.

To assess the relevance of our results, an analysis of variance (ANOVA) is applied. The corresponding results are shown in Tables 3 and 3 within the Appendix section. It is clear that the contribution on electrical efficiency, comes first from the fluid velocity (A) with a value of 55.40% with respect to the

Table 3. Factors chosen in the factorial design of ANOVA analysis.

Code	Factor	Level		
		(-)	(0)	(+)
A	Fluid velocity (m/s)	0.001	0.0255	0.05
B	Pipe length (m)	5	7.5	10
C	Pipe diamtre (m)	0.005	0.0075	0.01
D	Tube thickness (m)	0.0003	0.00165	0.003
E	Inlet fluid temperature (K)	283.15	293.15	303.15

overall variation of all effects and interactions (29,5707/53,3843). The second significant contribution comes from the pipe diameter (C) with 20.9%.

The third contribution comes from the second interaction between pipe length (B) and pipe diameter (C) with 11.95%. For the two-way interactions, the highest contribution comes from the interaction between the pipe length (B) and the pipe diameter (C), BC. The remaining contributions are shown in Table 2 within the Appendix section.

For the thermal efficiency, it is observed that the highest contribution comes from the fluid velocity (A) with a value of 72.5% with respect to the overall variation of all effects and interactions (13,985,6/19,285,5). This contribution is even higher than the one calculated for the electrical efficiency (55.40%), meaning that the fluid velocity has more effect on the thermal efficiency than the electrical one. The second contribution comes from the pipe diameter (C) with a value of 15.8%. Then, the contribution from the tube thickness (D) comes as the third one with a value of (4%). For the two-way interactions, the one between the pipe length (B) and the pipe diameter (C), BC, is the highest one (1.48%)

The effects of the main parameters on the electrical and thermal efficiency of the PV/T are plotted in Figure 2, 3. It is noticed in Figure 2 increasing the velocity of the refrigerant water (A) or the pipe diameter (C) increases the electrical efficiency. This is in agreement with the variance analysis where we found that the fluid velocity (A) is the parameter that affects the most the electrical efficiency. In addition, this behavior is in agreement with the one reported by (Nahar, Hasanuzzaman, and Rahim 2017b). The pipe length (B) is found to affect the electrical efficiency but to a lesser extent than the pipe diameter (C). In addition, increasing the pipe thickness has a positive effect until a maximum value of 0.00165 m. Then, the thickness of the pipe will have a decreasing effect on the electrical efficiency. Concerning the inlet fluid temperature (E), it has a negative effect on the electrical efficiency, in agreement with the results reported in (Bardhi, Grandi, and Tina 2012).

Figure 3 shows clearly that increasing the water velocity (A) and the pipe diameter (C) has positive effect on the thermal efficiency. In addition, the pipe length (B), pipe thickness (D) and the inlet fluid temperature (E) (Alobaid et al. 2018) have a negative effect on the thermal efficiency.

Figure 4, 5 presented the effect of the PV/T interactions parameters on the electrical and thermal efficiencies. The advantage of displaying the interaction effects plots is to show the

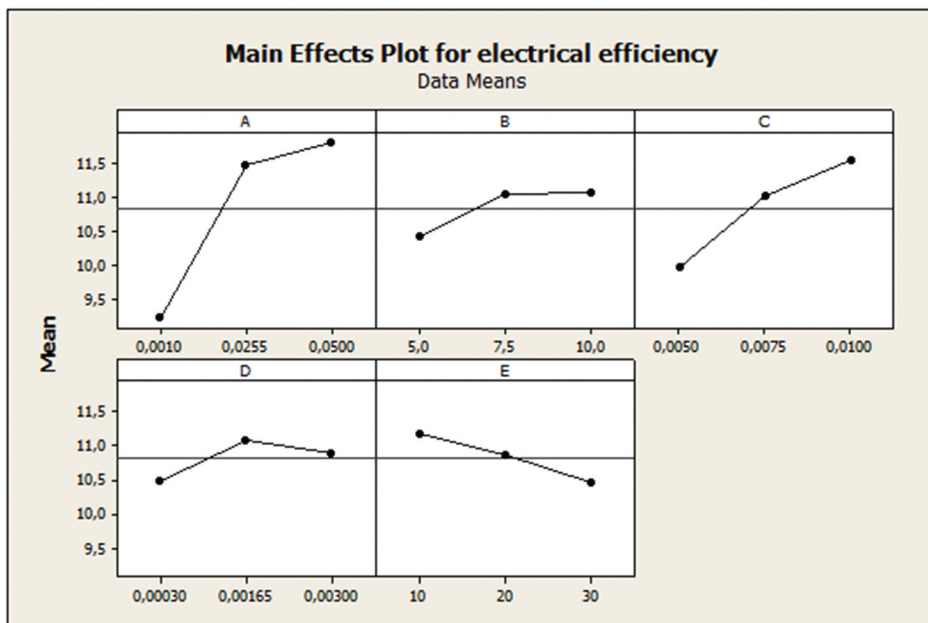


Figure 2. Main effect plots of PV/T parameters on the electrical efficiency.

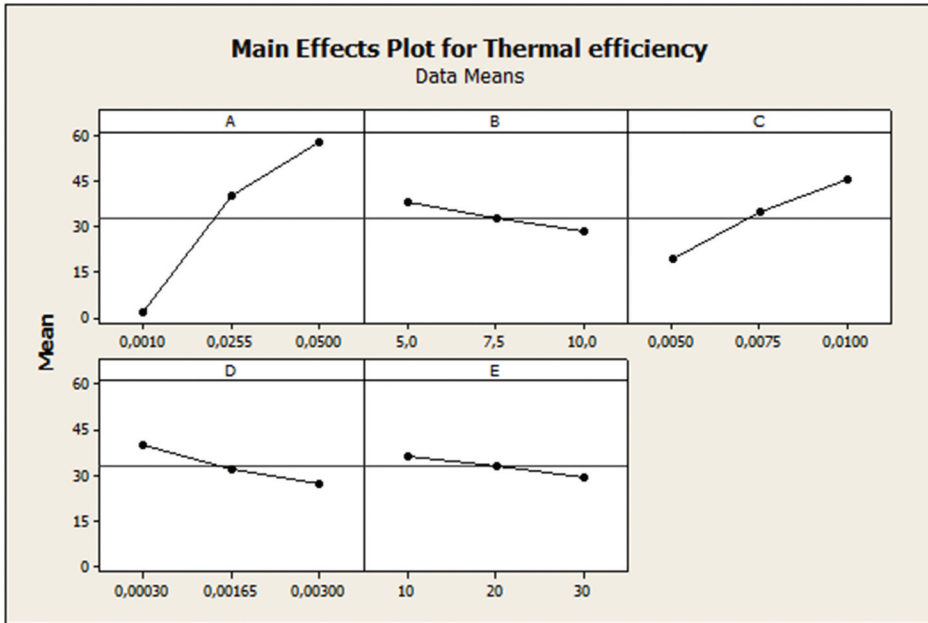


Figure 3. Main effect plots of PV/T parameters on the thermal efficiency.

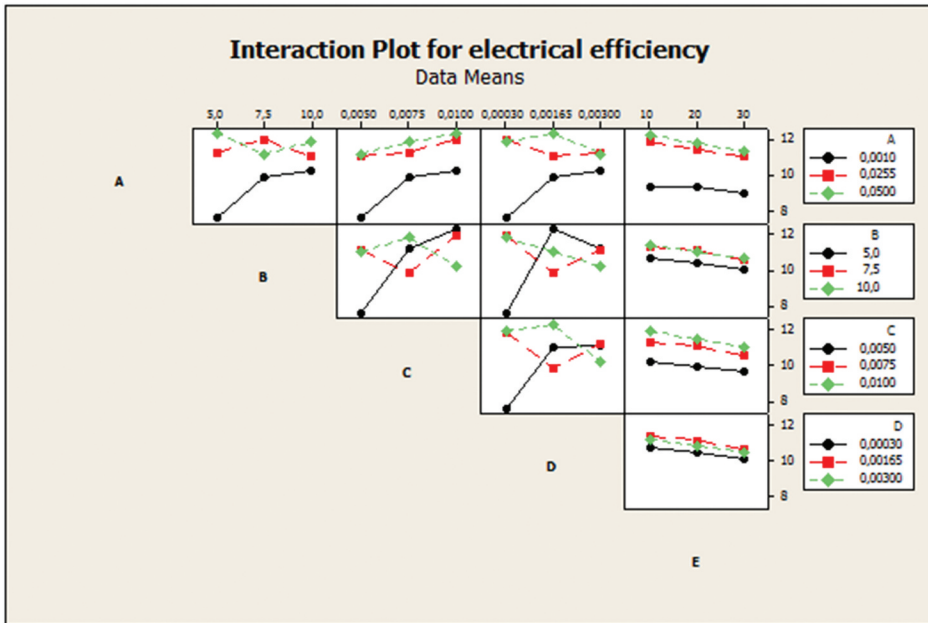


Figure 4. Interaction effect plots of the PV/T parameters on the electrical efficiency.

importance of the second categorical factors and how the relationship between these factors affect the electrical and thermal efficiencies. Each plot shows the variation of a factor at three levels by three lines (black, red and green) as a function of another varying factor on the x-axis. The y-axis represents the efficiency. In order to study the effect of each parameter on all the

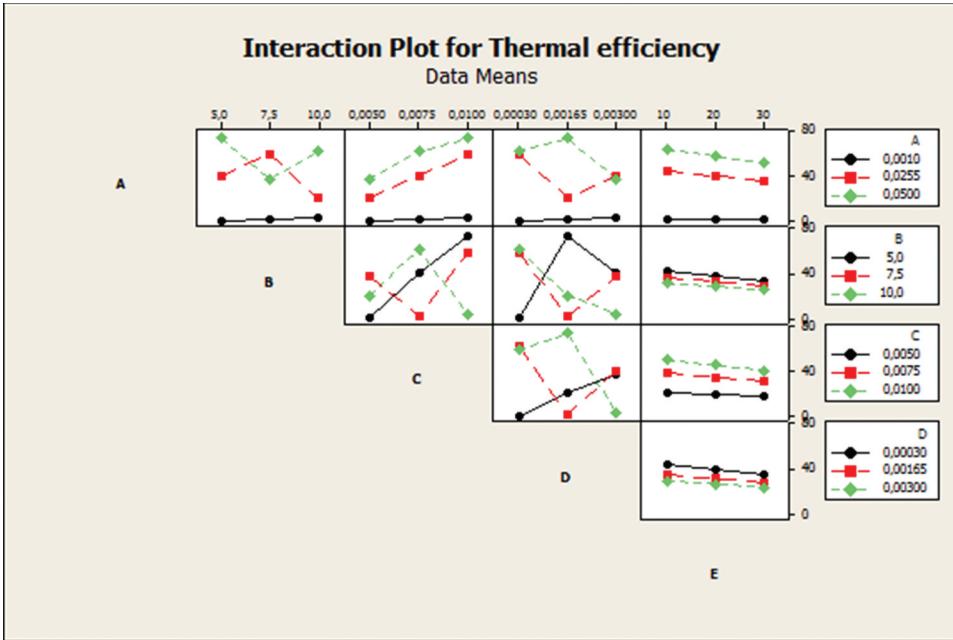


Figure 5. Interaction effect plots of PV/T parameters on the thermal efficiency.

other ones and the influence of the corresponding interactions on the electrical (Figure 4) and thermal (Figure 5) efficiencies, one parameter is fixed, changed each of all the others separately (panel rows) and calculated the efficiencies for each parameter combination. In the case where the lines are parallel, we would not have any interaction (J. Antony 2015; Terrab and Kara 2018). This is the case for the last column of Figures 4a and 4b, where the inlet fluid temperature (E) does not affect the fluid velocity (A), the pipe length (B), the pipe diameter (C), nor the pipe thickness (D) when it comes to either efficiencies. In other words, the electrical and thermal efficiencies are independent of the inlet fluid temperature (E) parameter/factor interaction with all the other parameters, A, B, C and D.

For the electrical efficiency, only considerable interaction effects are shown in Figure 4. When the velocity is 0,001 m/s (black circles), the electrical efficiency increases when increasing the pipe length (B), the pipe diameter (C), or the pipe thickness (D). However, for the same fluid velocity, we can easily notice that the electrical efficiency decreases when increasing the inlet fluid temperature (E). When the fluid velocity (A) is 0,0255 m/s (red squares), increasing the pipe length (B) increases the electrical efficiency to a maximum for which the length B is 7,5 m. Increasing the pipe diameter (C) increases the electrical efficiency as well. Increasing the pipe thickness (D), the electrical efficiency decreases to a minimum for which the thickness D is 0,00165 m. When the velocity is 0,05 m/s (green diamonds), increasing pipe length (B) decreases the electrical efficiency to a minimum for which the length B is 7,5 m. When increasing the pipe diameter (C) the electrical efficiency increases to a maximum for which the diameter C is 0,00165 m. Considering the interaction between the pipe diameter (C) and the pipe length (B), when the pipe length (B) is 5 m (black circles), the electrical efficiency increases when increasing the pipe diameter (C). However, when the pipe length (B) is 7,5 m (red squares), the electrical efficiency has a minimum at a diameter C of 0,0075 m. In addition, when the pipe length (B) is 10 m (green diamonds), the electrical efficiency has a maximum at the same diameter. If we consider now the interaction between the pipe length (B) and the pipe diameter (D), it can be seen from the plots that when the pipe length (B) is 5 m (black circles), the electrical efficiency has a maximum at a thickness D of 0,00165 m. When the pipe length (B) is 7,5 m (red squares), the electrical efficiency reaches the minimum at a thickness D of 0,00165 m. However, when the pipe length is 10 m (green diamonds), the electrical efficiency decreases

when increasing the pipe thickness (D). When it comes to the interaction between the pipe diameter (C) and the pipe thickness (D), we can say that when the pipe diameter (C) is around 0.005 m, the electrical efficiency increases when increasing the pipe thickness (D). However, When the pipe diameter (C) is around 0.0075 m, the electrical efficiency has a minimum at a pipe thickness (D) of 0,00165 m and when the pipe diameter (C) is around 0,01 m the electrical efficiency has a maximum at the same value of the pipe thickness (D).

As for the electrical efficiency, only considerable interaction effects are shown in Figure 5 for the thermal efficiency. When the fluid velocity (A) is 0,001 m/s (black circles) the thermal efficiency is constant whenever A is interacting with B, C, D, or E. This means that the thermal efficiency is independent of any interaction involving the fluid velocity (A). When the fluid velocity (A) is 0,0255 m/s (red squares), increasing pipe length (B) gives the thermal efficiency a maximum at a length B of 7,5 m. While increasing the pipe diameter (C) increases the thermal efficiency, increasing the pipe thickness (D) decreases the thermal efficiency to a minimum at thickness D of 0,00165 m. When the fluid velocity (A) is 0,05 m/s (green diamonds), increasing the pipe length (B) gives the thermal efficiency a minimum at length B of 7,5 m. When increasing the pipe diameter (C), the thermal efficiency increases and when increasing the pipe thickness (D) the thermal efficiency reaches a maximum at thickness D of 0,00165 m. For the aspect of the interaction between the pipe length (B) and the other effect parameters, C and D, it is observed that when the pipe length (B) is 5 m (black circles), the thermal efficiency increases when increasing the pipe diameter (C). However, when the pipe length (B) is 7.5 m (red squares), the thermal efficiency reaches a minimum at a diameter C of 0,0075 m. In addition, when the pipe length (B) is 10 m (green diamonds), the thermal efficiency reaches a maximum at a diameter C of 0,0075 m. When the pipe length (B) is 5 m (black circles), the thermal efficiency reaches a maximum at a thickness D of 0,00165 m, when the pipe length (B) is 7,5 meter (red squares), the thermal efficiency reaches a minimum at the same thickness D. However, when the pipe length is 10 m (green diamonds), the thermal efficiency decreases when increasing the pipe thickness (D). For the analysis of the interaction between the pipe diameter (C) and the pipe thickness (D). When the pipe diameter (C) is 0.005 m (black circles), the thermal efficiency increases when increasing the pipe thickness (D). However, when the pipe diameter (C) is 0.0075 m (red squares), the thermal efficiency reaches a minimum at thickness D of 0,00165 m and when the pipe diameter (C) is 0,01 m (green diamonds), the thermal efficiency reaches a maximum at a thickness D of 0,00165 m.

Data regression is used to estimate the relationships between dependent variables. These relationships can be considered as a mathematical model. In our case, using Appendix Table 1 as input, Minitab is used to calculate R^2 for electrical and thermal efficiencies in terms of A, B, C, D and E:

$$\begin{aligned} \text{Electrical efficiency}(\%) = & - 48.3964 + (307.012 \times A) + (1.26005 \times B) + 2070.52 \times C \\ & + (1217.25 \times D) + (0.313184 \times E) - (1556.76 \times A \times A) \\ & - (0.0474107 \times B \times B) - (43243.3 \times C \times C) - (216281 \times D \times D) \\ & - 4.99215 \times 10^{-4} \times E \times E - (0.597995 \times A \times E) \\ & - (0.00143253 \times B \times E) - 3.77667 \times C \times E - (1.20583 \times D \times E). \end{aligned}$$

Table 4. Material and thermal characteristics of the PV/T collector as used in(Nahar, Hasanuzzaman, and Rahim 2017b).

Materials	Layer	Thermal Density [kg/m ³]	ThermalConductivity [W/(mK)]	Heat capacity at constant pressure [J/kg K]	Thickness (mm)
Glass	Top cover	2450	2	500	3
EVA	Encapsulant	950	0.311	2090	0.8
Silicon	Solar cell	2329	148	700	0.1
Tedlar	Bottom cover	1200	0.15	1250	0.05
Thermal paste	Conductor	2600	1.9	700	0.3

$$R^2 = 0.9960.$$

$$\begin{aligned} \text{Thermal efficiency}(\%) = & -102.638 + (5494.82 \times A) - (8.93612 \times B) + (25663.5 \times C) \\ & - (20380 \times D) + (0.371491 \times E) - (17357.9 \times A \times A) \\ & + (0,0633153 \times B \times B) - (386664 \times C \times C) + (999409 \times D \times D) \\ & - (4.4678 \times 10^{-4} \times E \times E) - (11,8432 \times A \times E) + (0,0206423 \times B \times E) \\ & - (50,0043 \times C \times E) - (41,6478 \times D \times E). \end{aligned}$$

$$R^2 = 0.9997.$$

The process to determine the coefficient is also known as *R*-squared. On a convenient scale 0–1, it measures the strength of agreement between the results obtained from the model and simulations (Terrab and Kara 2018). R^2 is almost 1 in both cases; 0.9960 and 0.9997, meaning that this model is in agreement with the conducted simulations. Therefore, the factorial parameters; A, B, C, D and E being studied for electrical and thermal efficiencies are the most relevant ones and we can use these models to predict thermal and electrical efficiencies for PV/T systems in a defined interval of factors.

Results of the RSM calculations

The response surface optimizer is often used to find the optimal PV/T parameters combination that maximizes both electrical and thermal efficiency. The composite desirability is defined as the geometric mean of the individual desirability. The composite desirability, which represents the target response, is used to measure optimization success. The ideal situation corresponds to a desirability of one. Zero means that at least one value of the response is away from acceptable values (Terrab and Kara 2018). A CCD (Central Composite Design) with three levels is required to construct an RSM simulation (Leonzio 2019).

The factors and the corresponding levels are the same we used in the previous ANOVA analysis: fluid velocity (A), pipe length (B), pipe diameter (C), pipe thickness (D) and inlet water temperature (E).

The RSM optimization results of electrical and thermal efficiency are plotted in Figure 6. As it can be easily seen from this figure, the values that are highlighted in red; of the fluid velocity (0.05 m/s), the pipe length (7.27 m), diameter (0.01 m) and thickness (0.0008 m) and of the inlet fluid temperature (10 °C) are the optimal ones. Relying on the RSM results, we can say that these parameters characterize our PV/T system. In other words, we predict similar PV/T systems to have optimal efficiencies at around the optimal values found for A, B, C, E and E.

Validation

The numerical model accuracy and validity is assessed by comparing our results to those obtained by other researchers using the same model as implemented within COMSOL Multiphysics. The work reported by (Nahar, Hasanuzzaman, and Rahim 2017b) is utilized to conduct the comparative analysis. Table 4 and table appendix Table 4 summarize the properties of the PV/T taken from the publication of (Nahar, Hasanuzzaman, and Rahim 2017b)

Using these values as input data in our simulation, we found a total efficiency of 84%. Comparing this value to those calculated and experimentally extracted by (Nahar, Hasanuzzaman, and Rahim 2017b) of 84.4% and 80%, respectively, we can say that our calculation reproduced the numerical and the experimental values to a satisfactory extent. The choice of the work of (Nahar, Hasanuzzaman, and Rahim 2017b) was motivated by the relevance of the experimental investigation carried in this work.

The comparison demonstrates that our model is validated directly by simulation and indirectly by the experiment presented by (Nahar, Hasanuzzaman, and Rahim 2017b). This indicates that our simulations produce a predictive power strategy that can be utilized to stimulate future experiments.

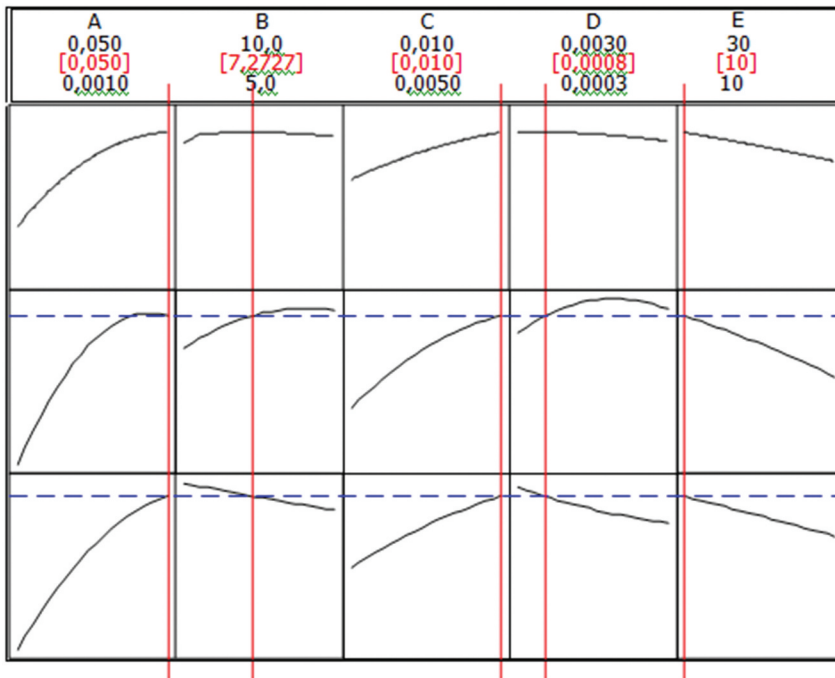


Figure 6. Response optimisation of the PV/T parameters (optimal values are highlighted in red).

Conclusion

In this work, we explored the influence of controllable parameters and factors on the efficiency of PV/T systems implemented within the region of Souk Ahras. Based on applying the statistical method of ANOVA, we have shown that the fluid velocity, the pipe diameter and the inlet fluid temperature are the most influential factors on the performance of generating electricity from PV/T systems. For the thermal efficiency, the length of the diameter is important in tandem with the previously mentioned parameters.

The conducted empirical analysis has confirmed the existence of strong interrelation between controllable parameters including fluid velocity and pipe length, pipe length and pipe diameter. Our results showed that to attain the maximum electrical efficiency for the system, the factors of fluid velocity, pipe length and pipe diameter should ideally reach the high level while the fluid temperature factor should inversely be at the low level and the pipe thickness should be at the intermediate level.

As for thermal efficiency, the optimum is that the factors: fluid velocity and pipe diameter should be high while the factors pipe length, pipe thickness and fluid temperature should be at low level.

The optimal operating conditions are found by applying the Response Surface Methodology (RSM) : the fluid velocity, the pipe length, diameter, thickness and the inlet fluid temperature are found to be around, 0.05 m/s, 7.27 m, 0.01 m, 0.0008 m, and 283.15 K, respectively.

According to the Response surface methodology RSM calculations, when the former factors Water velocity (A), pipe length (B), pipe diameter (C), pipe thickness (D) and inlet fluid temperature (E) are around the latter values, we expect the thermal and electrical efficiencies to be around 80.73% and 12.87%, respectively.

The proposed methodology provides an efficient and quick working tool for analyzing and optimizing the effect of various controllable parameters on photovoltaic/thermal performance without requiring excessive computational resources, saving money and time during the computational analysis. Furthermore, it can be efficiently extended for studying other factors. For the next milestone,

we plan to study how the performance of the PV/T is affected when replacing the fluid by a Nano-fluid or a phase change materials (PCM).

Disclosure statement

No potential conflict of interest was reported by the author(s).

ORCID

Ilias Terrab  <http://orcid.org/0000-0002-1342-2427>

Nomenclature

A_c	PV cell area (m ²)
A_{fc}	Cross-sectional area of the inlet flow channel (m ²)
C_p	Specific heat capacity at constant pressure (J kg ⁻¹ K ⁻¹)
C_{pw}	Specific heat capacity of water (J kg ⁻¹ K ⁻¹)
D_i	Inner diameter, m
E_c	Total solar energy absorbed into the cell, W
E_{el}	Electrical energy, W
E_{th}	Thermal energy extracted by water, W
h_c	Convection heat transfer coefficient, W/m ² K
k_s	Thermal conductivity of the solid, W/m K thermal
k_w	Thermal conductivity of water, W/m K mass
\dot{m}	Mass flow rate, kg/s
P	Pressure, Pa
R	Solar irradiance, W/m ²
T	Variable water temperature, °C
T_{amb}	Ambient temperature, °C
T_c	Temperature of PV cell, °C
T_{in}	Water inlet temperature, °C
T_{out}	Water outlet temperature, °C
T_{ref}	Reference cell temperature, °C
u, v, w	Components of velocity vector, m/s
u	Velocity vector field, m/s
U_0	Inlet water velocity, m/s
ANOVA	Analysis of variance
DOE	Design of Experiments Method
RSM	Response surface methodology
FEM	Finite Element Method

Greek symbols

β_{ref}	Temperature coefficient at reference cell temperature
ν	Kinematic viscosity of the water, m ² /s
ρ	Density of the water, kg/m ³
η_{Tref}	PV cell electrical efficiency at reference temperature
η_{th}	Thermal efficiency
η_{el}	Electrical efficiency
$\bar{\eta}_{el}$	Average electrical efficiency
η_{Tot}	Total PV/T efficiency
τ_g	Glass Emissivity
α_c	Absorptivity of PV cell

References

- Abdelrazik, A. S., F. A. Al-Sulaiman, R. Saidur, and R. Ben-Mansour. 2018, December. A review on recent development for the design and packaging of hybrid photovoltaic/Thermal (PV/T) solar systems. (2017) *Renewable and Sustainable Energy Reviews* 95:110–29. doi:10.1016/j.rser.2018.07.013.
- Abdullah, A. L., S. Misha, N. Tamaldin, M. Afzanizam Mohd Rosli, and F. Abdulameer Sachit. 2019. Hybrid photovoltaic thermal PVT solar systems simulation via Simulink/Matlab. *CFD Letters* 11 (4):64–78.
- Afroza, N., M. Hasanuzzaman, N. A. Rahim, and S. Parvin. 2019. Numerical investigation on the effect of different parameters in enhancing heat transfer performance of photovoltaic thermal systems. *Renewable Energy* 132:284–95. doi:10.1016/j.renene.2018.08.008.
- Alobaid, M., B. Hughes, D. O'Connor, J. Calautit, and A. Heyes. 2018. Improving thermal and electrical efficiency in photovoltaic thermal systems for sustainable cooling system integration. *Journal of Sustainable Development of Energy, Water and Environment Systems* 6 (2):305–22. doi:10.13044/j.sdewes.d5.0187.
- Antony, J. 2015. Taguchi or classical design of experiments : a perspective from a practitioner. *July* 2006. doi:10.1108/02602280610675519.
- Antony, A., Y. D. Wang, and A. P. Roskilly. 2019. A detailed optimisation of solar photovoltaic/thermal systems and its application. *Energy Procedia* 158 (2018):1141–48. doi:10.1016/j.egypro.2019.01.295.
- Bardhi, M., G. Grandi, and G. M. Tina. 2012. Comparison of PV cell temperature estimation by different thermal power exchange calculation methods, International Conference on Renewable Energies and Power Quality, 28th to 30th March, 2012, Santiago de Compostela (Spain), 1: 653–58.
- Brahim, T., and A. Jemni. 2017. Economical assessment and applications of photovoltaic/thermal hybrid solar technology: a review. *Solar Energy* 153:540–61. doi:10.1016/j.solener.2017.05.081.
- Cheikh El Hocine, H. B., A. Gama, and K. Touafek. 2018. The feasibility of new design of hybrid photovoltaic-thermal system—a theoretical approach. *International Journal of Ambient Energy* 39 (5):496–507. doi:10.1080/01430750.2017.1318778.
- Das, D., and P. Kalita. 2020. Experimental analysis of photovoltaic-thermal collectors with closely spaced tubes. *Energy Sources, Part A: Recovery, Utilization and Environmental Effects* 00 (00):1–23. doi:10.1080/15567036.2020.1814904.
- Deng, H., X. Yang, R. Tian, J. Hu, B. Zhang, and F. Cui. 2020, April. Modeling and optimization of solar thermal-photovoltaic vacuum membrane distillation system by response surface methodology. (2017) *Solar Energy* 195:230–38. doi:10.1016/j.solener.2019.11.006.
- “Detailed explanation of the Finite Element Method (FEM).” n.d. Accessed April 30, 2021. <https://www.comsol.com/multiphysics/finite-element-method>.
- Dutreuil, J. A., and H. A. Hadim. 2017. DESIGN PARAMETERS FOR HIGH-EFFICIENCY HYBRID PV/THERMAL SOLAR ENERGY SYSTEMS, ASME/JSME 2011 8th Thermal Engineering, March 13-17, 2011, Honolulu, Hawaii, USA. 1–9.
- Dutta, S. 2017. “*Optimization in Chemical Engineering*”. England: Cambridge University Press.
- Fazlay, R., R. Khairul Habib, S. N. Aslfattahi, S. Mohd Yahya, L. Das, and L. Das. 2020. Performance optimization of a hybrid PV/T solar system using soybean oil/mxene nanofluids as a new class of heat transfer fluids. *Solar Energy* 208 (May):124–38. doi:10.1016/j.solener.2020.07.060.
- Fontenault, B. J., and E. Gutierrez-Miravete. 2012. “Modeling a combined photovoltaic-thermal solar panel.” *COMSOL Conference*, Boston, 1–8.
- Geiger, E. O., and G. Algorithm, RespoNse surface, loss prevention, and artificial neural network. n.d. “Optimization Statistical Methods for Fermentation Response Surface Methodology.”
- Gelis, K., K. Ozbek, A. Naci Celik, and O. Ozyurt May 2022. A novel cooler block design for photovoltaic thermal systems and performance evaluation using factorial design. *Journal of Building Engineering* 48:103928. doi:10.1016/J.JOBE.2021.103928.
- Gomaa, M. R., M. Ahmed, and H. Rezk. 2022. Temperature distribution modeling of PV and cooling water pv/t collectors through thin and thick cooling cross-fined channel box. *Energy Reports* 8:1144–53. doi:10.1016/j.egy.2021.11.061.
- Herez, A., H. El Hage, T. Lemenand, M. Ramadan, and M. Khaled February 2020. Review on photovoltaic/thermal hybrid solar collectors: classifications, applications and new systems. *Solar Energy* 207:1321–47. doi:10.1016/j.solener.2020.07.062.
- Jonas, D., M. Lämmle, D. Theis, S. Schneider, and G. Frey. 2019. Performance modeling of PVT collectors : Implementation, validation and parameter identification approach using TRNSYS. 193 (September):51–64. doi:10.1016/j.solener.2019.09.047.
- Kalkan, C., and M. Akif. 2019. Numerical study on photovoltaic/thermal systems with extended surfaces. *Wiley Energy Research* 1–17. 2018. November. doi:10.1002/er.4477.
- Kazemian, A., M. Khatibi, T. Ma, and T. Ma. 2021. Performance prediction and optimization of a photovoltaic thermal system integrated with phase change material using response surface method. *Journal of Cleaner Production* 290:125748. doi:10.1016/j.jclepro.2020.125748.
- Kazemian, A., A. Parcheforosh, A. Salari, and T. Ma. 2021, May. Optimization of a novel photovoltaic thermal module in series with a solar collector using Taguchi based grey relational analysis. (2020) *Solar Energy* 215:492–507. doi:10.1016/j.solener.2021.01.006.

- Khuri, A. I., and S. Mukhopadhyay. 2010. Response Surface Methodology. *Wiley Interdisciplinary Reviews Computational Statistics* 2 (2):128–49. doi:10.1002/wics.73.
- Lateef, A., S. Misha, N. Tamaldin, M. A. M. Rosli, and A. Sachit January 2020. Case studies in thermal engineering theoretical study and indoor experimental validation of performance of the new photovoltaic thermal solar collector (PVT) based water system. *Case Studies in Thermal Engineering* 18:100595. doi:10.1016/j.csite.2020.100595.
- Leonzio, G. 2019. Modelling and optimisation the efficiency of crystalline silicon PV/T solar panel. *International Journal of Sustainable Energy* 38 (8):716–39. doi:10.1080/14786451.2019.1584626.
- Marudaipillai, S. K., B. Karuppudayar Ramaraj, R. Kumar Kottala, and M. Lakshmanan. 2020. Experimental study on thermal management and performance improvement of solar PV panel cooling using form stable phase change material. *Energy Sources, Part A: Recovery, Utilization and Environmental Effects* 00 (00):1–18. doi:10.1080/15567036.2020.1806409.
- Montgomery, D. C. 2005. *Design and Analysis of Experiments*. New York, NY: John Wiley & Sons.
- Moradi Kamran, M., A. Ebadian, and C. Xian Lin. 2013. A review of PV/T technologies: Effects of control parameters. *International Journal of Heat and Mass Transfer* 64:483–500. doi:10.1016/j.ijheatmasstransfer.2013.04.044.
- Nahar, A., M. Hasanuzzaman, and N. A. Rahim. 2017a. A Three-Dimensional comprehensive numerical investigation of different operating parameters on the performance of a photovoltaic thermal system with pancake collector. *Journal of Solar Energy Engineering, Transactions of the ASME* 139 (3):3. <https://doi.org/10.1115/1.4035818>.
- Nahar, A., M. Hasanuzzaman, and N. A. Rahim. 2017b. Numerical and experimental investigation on the performance of a photovoltaic thermal collector with parallel plate flow channel under different operating conditions in Malaysia. *Solar Energy* 144:517–28. doi:10.1016/j.solener.2017.01.041.
- Numan, A., and F. Kaya. 2020. Experimental thermodynamic analysis of air-based PVT system using Fi Ns in Di Ff Erent Materials : Optimization of control parameters by Taguchi method and ANOVA. 197. November2019199–211. doi:10.1016/j.solener.2019.12.077.
- Obalanlege, M. A., Y. Mahmoudi, R. Douglas, E. Ebrahimnia-, J. Davidson, and D. Bailie. 2019. Performance assessment of a hybrid photovoltaic-thermal and heat pump system for solar heating and electricity. *Renewable Energy Elsevier Ltd.* doi:10.1016/j.renene.2019.10.061.
- Pang, W., B. C. Duck, C. J. Fell, G. J. Wilson, W. Zhao, and H. Yan January 2021. Influence of multiple factors on performance of photovoltaic-thermal modules. *Solar Energy* 214:642–54. doi:10.1016/j.solener.2020.11.050.
- Rahman, M. M., M. Hasanuzzaman, and N. A. Rahim. 2015. Effects of various parameters on PV-module power and efficiency. *Energy Conversion and Management* 103:348–58. doi:10.1016/j.enconman.2015.06.067.
- Ramdani, H., and C. Ould-Lahoucine May 2020. Study on the overall energy and exergy performances of a novel water-based hybrid photovoltaic-thermal solar collector. *Energy Conversion and Management* 222:113238. doi:10.1016/j.enconman.2020.113238.
- Rejeb, O., C. Ghenai, M. Hedi Jomaa, and M. Bettayeb. 2020. Statistical study of a solar nanofluid photovoltaic thermal collector performance using response surface methodology. *Case Studies in Thermal Engineering* 21: 100721. doi:10.1016/j.csite.2020.100721
- Sachit, F. A., N. Tamaldin, M. A. M. Rosli, S. Misha, and A. L. Abdullah. 2018. Current progress on flat-plate water collector design in photovoltaic thermal (PV/T) systems: A review. *Journal of Advanced Research in Dynamical and Control Systems* 10 (4):680–89.
- Sainthiya, H., and N. Singh Beniwal. 2020. Comparative analysis of electrical performance parameters under combined water cooling technique of photovoltaic module: An experimental investigation. *Energy Sources, Part A: Recovery, Utilization and Environmental Effects* 42 (15):1902–13. doi:10.1080/15567036.2019.1604894.
- Sathyamurthy, R., and S. W. Sharshir. 2020. Photovoltaics performance improvement using different cooling methodologies: A state-of-art review. *Journal of Cleaner Production* 122772. doi:10.1016/j.jclepro.2020.122772.
- Shen, C., F. Liu, S. Qiu, X. Liu, F. Yao, and Y. Zhang. 2021, July. Numerical study on the thermal performance of photovoltaic thermal (PV/T) collector with different parallel cooling channels. (2020) *Sustainable Energy Technologies and Assessments* 45:101101. doi:10.1016/j.seta.2021.101101.
- Shuang-Ying, W., Q.-L. Zhang, L. Xiao, and F.-H. Guo. 2011. A heat pipe photovoltaic/Thermal (PV/T) hybrid system and its performance evaluation. *Energy & Buildings* 43 (12):3558–67. doi:10.1016/j.enbuild.2011.09.017.
- Silva, R. M. D., and J. L. M. Fernandes. 2010. Hybrid photovoltaic/Thermal (PV/T) solar systems simulation with Simulink/Matlab. *Solar Energy* 84 (12):1985–96. doi:10.1016/j.solener.2010.10.004.
- Tata, O., M. Feddaoui, and Y. Belkassmi. 2018. “Numerical study on energy performance of sheet and tube type photovoltaic thermal solar system.” *AIP Conference Proceedings* 2056(December). doi:10.1063/1.5084994.
- Terrab, H., and A. Kara. 2018. Parameters design optimization of 230 KV corona ring based on electric field analysis and response surface methodology. *Electric Power Systems Research* 163:782–88. doi:10.1016/j.ejpsr.2017.06.002.
- Touafek, K., M. Haddadi, and A. Malek. 2013. Design and modeling of a photovoltaic thermal collector for domestic air heating and electricity production. *Energy & Buildings* 59:21–28. doi:10.1016/j.enbuild.2012.10.037.
- Valeriu, S., B. Hajji, C. El Fouas, and N. Cristian Chereches. 2022. Applied sciences numerical and parametric analysis for enhancing performances of water photovoltaic/thermal system. *Applied Sciences* 12: 646.